NRC Research Press

ARTICLE

Development of an early-warning time-of-failure analysis methodology for open-pit mine slopes utilizing ground-based slope stability radar monitoring data

Graham J. Dick, Erik Eberhardt, Albert G. Cabrejo-Liévano, Doug Stead, and Nick D. Rose

Can. Geotech. J. Downloaded from www.nrcresearchpress.com by University of British Columbia on 04/09/15
For personal use only.

Abstract: The recent introduction of ground-based slope stability radar in open-pit mines to complement conventional geodetic monitoring programs provides near real-time deformation measurements over a broad coverage area; this allows geotechnical engineers to observe the spatial distribution of pit wall movements and their progression over time. This paper presents a newly proposed early warning time-of-failure (TOF) analysis procedure for use in real-time with ground-based radar measurements designed to be integrated in an open-pit mine's trigger action response plan (TARP). The inverse-velocity and slope gradient (SLO) TOF analysis methods are applied to radar displacement measurements using a new systematic multi-pixel selection technique termed the "percent deformation method." The utilization of the percent deformation method in the proposed real-time TOF analysis methodology gives more-reliable results than current practice by providing recommendations for pixel selections, data filtering, where and how to undertake TOF analyses, and presenting TOF results in real time. The addition of a more rigorous, methodical treatment of radar monitoring data when faced with critical slope instability will reduce uncertainty and increase confidence in any trigger action response decisions, helping to ensure a safer work environment.

Key words: slope stability radar, inverse-velocity method, slope failure prediction, displacement monitoring, trigger action response plans.

Résumé : En association avec les méthodes conventionnelles, l'utilisation de radar basé au sol pour la surveillance des versants d'une mine à ciel ouvert a récemment permis aux ingénieurs géotechniciens d'obtenir des mesures presque instantanées de la distribution spatiale des mouvements à la surface et leur évolution temporelle sur une vaste région de couverture. Cet article présente une nouvelle procédure d'analyse basée sur l'utilisation du radar au sol pour annoncer en temps réel la rupture d'une pente (TOF) et déclencher le plan d'urgence spécifique de la mine. La méthode de la vitesse inversée ainsi que la méthode SLO TOF sont appliqués aux mesures de déplacement fournis par le radar en utilisant une nouvelle approche de sélection multi-pixel appelée « méthode du pourcentage de déformation ». L'utilisation de cette méthode intégrée à une analyse TOF en temps réel permet d'obtenir des résultats plus fiables par rapport aux approches habituelles utilisées pour la sélection des pixels, le filtrage des données, le choix de l'analyse TOF et la communication en temps réel des résultats. Lors d'instabilités critiques, l'intégration de cette méthode de traitement plus rigoureuse et systématique des données radar permet de réduire l'incertitude et accroît la fiabilité des décisions concernant l'activation d'un plan d'urgence améliorant ainsi la sécurité sur le travail dans les mines à ciel ouvert.

Mots-clés : radar basé au sol, méthode de la vitesse inversée, prédiction de rupture de pente, surveillance de déplacement, plans d'urgence spécifique.

Introduction

Ground-based radar is a remote sensing technology that uses phase-change interferometry to measure the surface deformation of a slope over time. The addition of ground-based radar to conventional geodetic prism monitoring programs in open-pit mines has enhanced active monitoring of unstable slopes. Published examples of successful implementation include the Leinster Nickel Mine (Cahill and Lee 2006), Potgietersrust Platinum Mine (Little 2006), Tom Price Mine (Day and Seery 2007), Barrick Goldstrike Mine (Armstrong and Rose 2009), Bingham Canyon Mine (Doyle and Reese 2011), Kemess South Mine (Yang et al. 2011), Grasberg Open Pit (Ginting et al. 2011), Wallaby Mine (Jones et al. 2011), and Savage River Mine (Macqueen et al. 2013). Ground-based radar provides three main advantages over traditional geodetic point monitoring: (*i*) broad slope coverage area, (*ii*) near real-time slope deformation data, and (*iii*) remote measurements without the need to install prism reflectors, reducing worker exposure to rock-fall hazards. Slope deformation alarms can be set within the radar scan area to alert mine operators to changes in pit wall behaviour. These alarms can be incorporated into the mine's trigger action response plan (TARP), which lays out pre-determined responses to likely events based on alert levels prompted by exceeding certain thresholds (Read and Stacey 2009).

Ground-based radars provide a line-of-site deformation point (or pixel) cloud with measurements updated every few minutes

Received 26 January 2014. Accepted 29 July 2014.

G.J. Dick* and E. Eberhardt. Geological Engineering, Department of Earth, Ocean, and Atmospheric Sciences, The University of British Columbia, 2020 – 2207 Main Mall, Vancouver, BC V6T 1Z4, Canada.
A.G. Cabrejo-Liévano. GroundProbe Pty Ltd., 72 Newmarket Road, Windsor, QLD 4030, Australia.
D. Stead. Department of Earth Sciences, Simon Fraser University, 8888 University Drive, Burnaby, BC V5A 1S6, Canada.
N.D. Rose. Piteau Associates Engineering Ltd., Suite 300-788 Copping Street, North Vancouver, BC V7M 3G6, Canada.
Corresponding author: Graham J. Dick (e-mail: gdick@bgcengineering.ca).
*Present address: BGC Engineering Inc., 234 St. Paul St., Kamloops, BC V2C 6G4, Canada.

Can. Geotech. J. Downloaded from www.nrcresearchpress.com by University of British Columbia on 04/09/15
For personal use only.

(Harries et al. 2006). This allows the geotechnical engineer to see the distribution of slope surface deformation behaviour within the scan area and its progression over time. However, when an accelerating slope deformation trend is detected, common practice involves arbitrarily selecting a single or small cluster of pixels for analysis rather than systematically utilizing the full spatial coverage provided by the radar (e.g., Cahill and Lee 2006; Little 2006; Day and Seery 2007; Harries and Roberts 2007).

This arbitrary pixel selection practice is based on the conventional application of time-of-failure (TOF) methods; for example, the inverse-velocity method (Fukuzono 1985) and the slope gradient (SLO) method (Mufundirwa et al. 2010), which were developed based on point measurement data. Periodic surveys of monitoring points would be analyzed for accelerations and extrapolated to predict impending failure. However, analyzing single points or a series of points can be precarious as uncertainties related to rock mass heterogeneity and complex failure modes can be misinterpreted. For example, an instability may collapse retrogressively rather than as one coherent event. To overcome these limitations, a procedure is required to fully utilize the near real-time full spatial area data provided by radar to perform TOF analyses.

Presented here is a real-time TOF analysis methodology derived from an investigation of eight large open-pit slope failures captured by a GroundProbe Slope Stability Radar (SSR); details are provided in Dick (2013). These cases represent a diverse sampling of open operations from around the world involving different slope heights, geology, and rock mass conditions. Incorporated in the real-time TOF analysis methodology is a new multi-pixel selection procedure, termed "the percent deformation method," developed for ground-based radar data. The methodology utilizes the inverse-velocity and SLO TOF methods. "Life expectancy" plots (Mufundirwa et al. 2010) are used to present the TOF results as they enable easy updating in real time as new deformation monitoring data are obtained.

The proposed real-time TOF analysis methodology is designed to be incorporated into a mine's TARP and be initiated when a slope deformation alarm has been triggered and (or) an accelerating deformation behaviour has been observed in the radar monitoring data. The developed methodology can also be applied to other rock slope hazards where radar monitoring is employed; for example, those threatening transportation corridors and landslides above dams. The objective is to improve the decision confidence of geotechnical engineers by providing a more rigorous methodology for conducting TOF analyses in times of heightened alert that optimizes the full advantages of near real-time and full spatial area deformation measurements provided by ground-based radar.

Background

Time-of-failure (TOF) analysis methods

Two TOF analysis methods were assessed in this research: the inverse-velocity method (Fukuzono 1985) and the SLO method (Mufundirwa et al. 2010). Both methods employ linear regression trends using time–deformation rate (velocity) measurements. "Life expectancy" plots (Mufundirwa et al. 2010) were used to present the TOF analysis results for both methods.

Fukuzono (1985) found that the time to accelerating creep failure under gravity loading was inversely proportional to the deformation rate (velocity). By plotting the inverse velocity versus time curve, one can estimate the TOF by extrapolating the trend to the x-axis (inverse velocity = 0). The reader is referred to Crosta and Agliardi (2003) for a detailed discussion of the technique applied to natural rock slopes. Rose and Hungr (2007) applied the inverse-velocity method to geodetic prism data, successfully predicting the time of slope failure in three hard-rock open-pit mines that occurred between 2001 and 2005. They observed that the inverse velocity often approaches linearity, especially close to the time of failure, and recommend the use of linear fits updated on an ongoing basis using the latest available deformation data. Venter et al. (2013) report subsequent attempts to apply the inverse-velocity method to open-pit mine slopes at the Tom Price Mine in Australia using prism data, but with mixed results. They found that although the inverse-velocity analysis allowed some interpretation to be made regarding deformation trends, the scatter present in the point measurement data prevented a useful prediction.

Mufundirwa et al. (2010) developed a method to analyze the time of geomechanical failure based on the slope (gradient) of the $t(du/dt)$–du/dt plot, where t is time and du/dt is the deformation rate. Mufundirwa et al. (2010) derived this relationship based on the strain divergence in the terminal phase of creep failure in rocks proposed by Fukui and Okubo (1997). This led to their development of "life expectancy" plots, which are used later in this paper to present the TOF analysis results for both the SLO and inverse-velocity methods. Venter et al. (2013) also applied the SLO method in their study of open-pit slope failures at the Tom Price Mine, and found that the method was very sensitive to data-averaging for velocity calculation as well as the data period used in the slope calculation. As a result, the TOF predictions produced varied significantly from day to day, either over- or under-predicting the TOF.

A key factor contributing to the problem of data scatter reported by Venter et al. (2013), in applying both the inverse-velocity and SLO methods, was likely their reliance on point measurement data. For the two slope failures analyzed in their study, the data was based on a small number of geodetic prisms (four), which were taken to be representative of the unstable slope area covering slope heights of up to 170 m.

Ground-based slope stability radar

Ground-based slope stability radar systems remotely measure the surface deformation of a slope from a stationary platform without the need for reflectors or prisms (Reeves et al. 2001). The system scans a region of the slope and divides the area of interest into pixels. The amount of movement is measured for each pixel and compared with the amount of movement from the previous scan. Remote monitoring using ground-based radar allows for active monitoring of a slope with deformation alerts of submillimetre precision, making the data available for interpretation usually within minutes (Harries et al. 2006) and without adverse effects from rain, fog, dust or smoke (Harries and Cabrejo 2010). Increasingly, ground-based radar systems are being integrated into the slope monitoring and management programs of most major open-pit mines. For example, Grasberg Mine's monitoring network utilizes GPS, extensometer, total station (prisms), and ground-based radar (Ginting et al. 2011).

Eight slope failures captured by a GroundProbe SSR system was used in this research. Figure 1 shows the SSR measurements of a single pixel from one of these slope failure cases. The deformation plot provides the cumulative horizontal slope displacement (between the SSR and the slope) with each progressive scan starting from the beginning of deployment. The amplitude is the signal strength of the reflection from the slope face. The range is the distance between the SSR dish and the slope. The coherence is a correlation measurement based on the range and amplitude between the current scan and the immediately preceding scan, with values close to 1.0 indicating little difference in range and amplitude between the two scans. The coherence measurement is especially useful for establishing the time of slope collapse. The coherence plot in Fig. 1 shows a downward spike to a coherence of approximately 0.1. This indicates a large difference in range and amplitude between the two scans, which coincides with the peak deformation and slope collapse.

The dimensions (or size) of a pixel depend on how far the SSR is placed from the slope; higher pixel resolution (smaller pixels) is achieved the closer the SSR is setup to the slope. When more than one pixel is selected, the deformation for the area of pixels is

Can. Geotech. J. Downloaded from www.nrcresearchpress.com by University of British Columbia on 04/09/15
For personal use only.

Fig. 1. Slope failure measurements captured by a GroundProbe SSR: theoretical cumulative deformation, deformation rate, and inverse velocity versus time plots illustrating the time of onset-of-acceleration, trend update point, and slope failure.

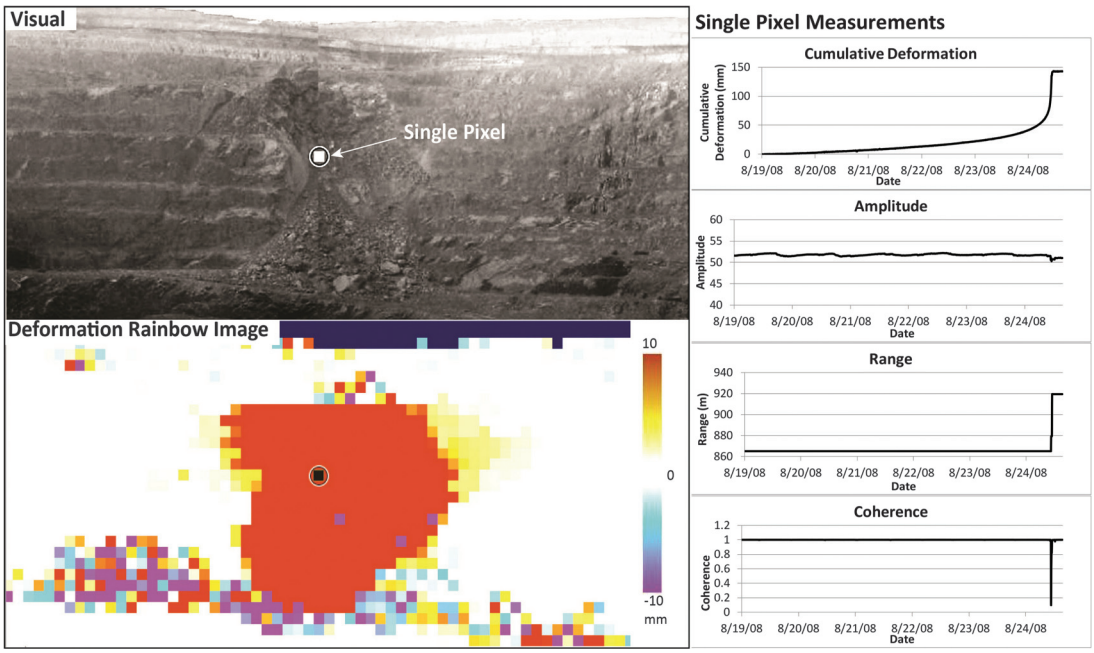

based on an amplitude-weighted average, which gives priority to the deformation of pixels that have a stronger return signal (GroundProbe Pty Ltd. 2012).

Trigger-action-response plan (TARP)

In conjunction with pit slope monitoring, whether by radar or in combination with conventional monitoring techniques, is the requirement for a TARP. TARPs prescribe pre-determined responses to likely alarm events, specifying which mine personnel are responsible for which responses. These characteristics vary between mine sites, but typically include alert levels (e.g., green, yellow, orange, red) for different conditions of the pit slope with specified responses by mine managers, superintendents, shift supervisors, geotechnical engineers and (or) mine workers for each alert level. A detailed example is provided by Read and Stacey (2009).

Alert levels are typically a function of the pit slope conditions and can be based on visual assessments, rate of slope movement, and acceleration observations (Read and Stacey 2009). Deformation thresholds can be established using ground-based radar to be included in a mine's TARP. Together, SSR and TARPs represent an important part of the ground control management responsibilities at many open-pit mining operations. This is reflected in the slope hazard management framework developed by Harries and Roberts (2007), who point to SSR as having led to a radical change in the management of risks in open-pit mining since its development in 2001.

Real-time "time-of-failure" (TOF) analysis methodology

The following subsections outline a TOF analysis methodology designed specifically for use with ground-based radar measurements. The methodology utilizes the real-time nature of SSR data, accounting for new slope deformation measurements being provided every few minutes. Figure 2 presents a flowchart of the developed real-time TOF analysis methodology. This section goes through and describes in detail each step of the methodology as presented in Fig. 2. A back-analyzed slope failure case study in an undisclosed open-pit copper mine is used throughout to illustrate the application of each step in the methodology.

Method terminology

Numerous authors use different nomenclature interchangeably when discussing slope instabilities. For example, the term "failure" has been applied in the literature to describe almost every stage in the evolution of slope instability leading to collapse (Mercer 2006). For the purpose of the methodology developed, the definitions presented in Table 1 are used. The terminology has been chosen to be consistent with that commonly used for engineered slopes in open-pit mines.

Two additional terms are also introduced: (*i*) the onset-of-acceleration (OOA) is used instead of the onset-of-failure (OOF) defined by Zavodni and Broadbent (1980), as an instability demonstrating accelerating behaviour may not necessarily result in a collapse; and (*ii*) a trend update (TU) point is specific to the use of real-time data. The deformation measurements provided by ground-based radar are updated every few minutes allowing for the identification of subtle trend changes. In addition, the noise in the radar measurements will typically decrease closer to slope failure. Therefore, defining a TU point allows older measurements to be substituted in favour of more recent, less noisy deformation trends in an effort to increase the accuracy of the TOF analysis closer to impending failure.

Figure 3 visually defines the OOA, TU, and slope failure points on cumulative deformation, deformation rate, and inverse velocity versus time plots. The slope failure point is taken at the end of the progressive (or accelerating) deformation stage and typically coincides with a major acceleration event in which integrity of the slope is lost, transitioning to regressive (or stable) levels marking the end of the failure event. Slope collapse is defined when material physically detaches from the slope. Depending on the nature of the rock mass (brittle or ductile), the time of slope collapse may not be exactly the same as slope failure.

Benchmark pixel and 50% deformation increment selection

The first step in the real-time TOF analysis method involves responding to a triggered SSR alarm or indications of slope instability (e.g., appearance of tension cracks), for which a benchmark pixel in the radar data is established (see top of Fig. 2). Two methods are recommended for selecting the benchmark pixel

Can. Geotech. J. Downloaded from www.nrcresearchpress.com by University of British Columbia on 04/09/15
For personal use only.

Fig. 2. Flowchart for the real-time time-of-failure analysis methodology.

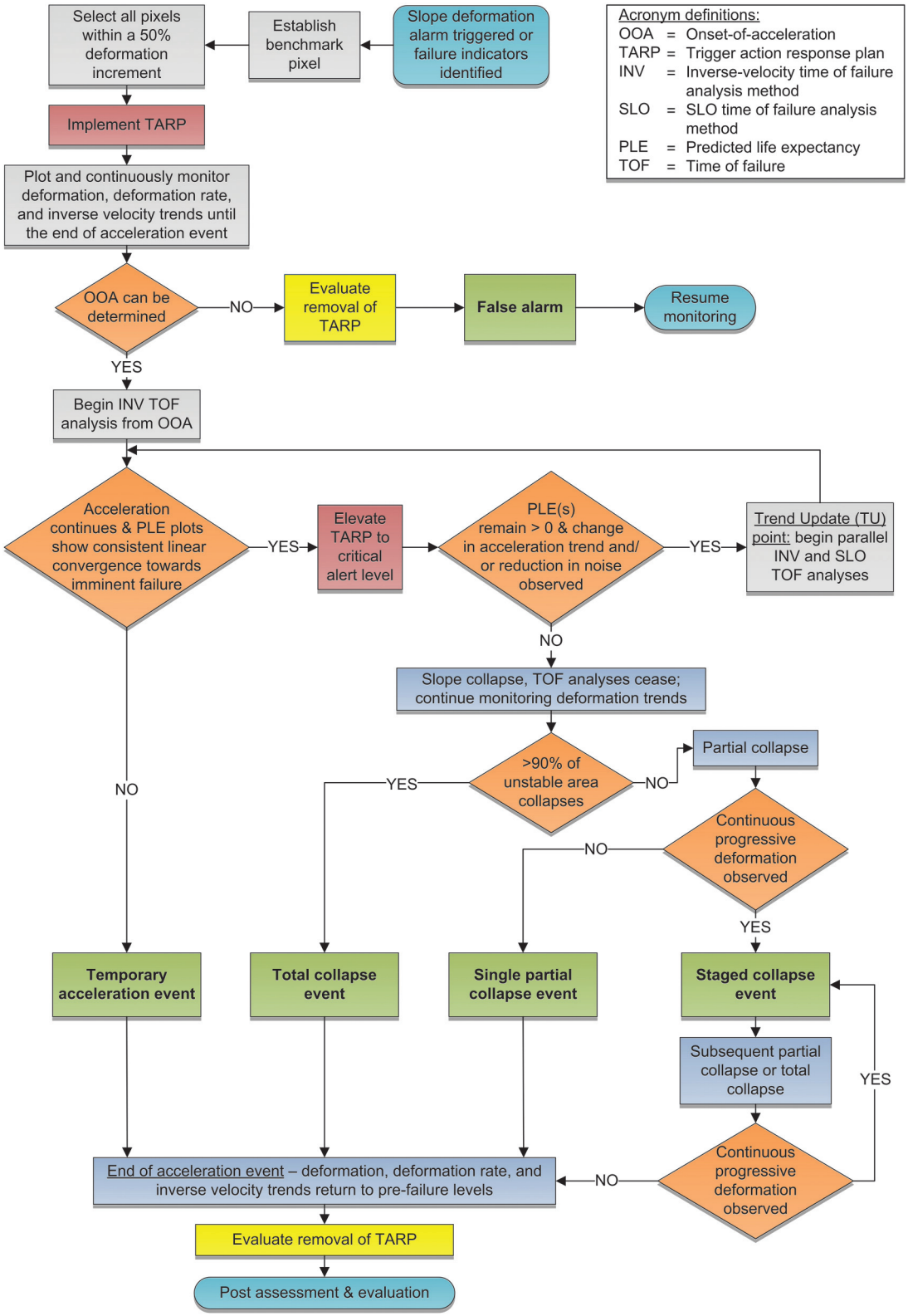

1. Use the pixel that triggered the slope deformation alarm; or
2. Take the pixel with the highest accumulated deformation if an acceleration trend is observed, but the alarm has not yet been triggered.

The latter ensures that observations from geotechnical staff are being considered as a check against the trigger threshold set.

A systematic multi-pixel selection technique is then implemented, termed "the percent deformation method", where mul-

Can. Geotech. J. Downloaded from www.nrcresearchpress.com by University of British Columbia on 04/09/15
For personal use only.

Table 1. Nomenclature for unstable slopes used in this study.

Term	Definition
Instability	Deformational movement or behaviour that does not involve collapse or failure (Mercer 2006).
Progressive deformation	Accelerating behaviour leading eventually to slope collapse (Zavodni and Broadbent 1980).
Regressive deformation	Decelerating behaviour leading eventually to a stable slope (Zavodni and Broadbent 1980).
Onset-of-acceleration (OOA)	Point defining the transition from a regressive state to an acceleration stage.
Trend update (TU) point	Point marking a change in the accelerating deformation trend and (or) a considerable decrease in noise within the progressive deformation stage.
Slope failure	Point where significant irreversible deformations (short of total collapse) result in the slope no longer being able to meet its design purpose; this is taken at the end of the progressive deformation stage.
Slope collapse	Physical, complete overall loss of rock mass integrity and structure (Mercer 2006).
Predicted life expectancy	Difference between the predicted time-of-failure and the time the prediction is made (Mufundirwa et al. 2010).

tiple pixels are selected based on a percentage of the deformation of the benchmark pixel; see Dick et al. (2013) for a detailed description. Two data trends are subsequently analyzed and compared throughout the implementation of the method: the single benchmark pixel and the 50% deformation increment. This is recommended because instabilities may or may not fail as one coherent mass. It is therefore essential that the first episode of slope collapse is forecast as accurately and reliably as possible while maintaining an understanding of the overall time-dependent behaviour of the rock mass over the entire instability during the failure event. The rationale behind using the benchmark, even though it is a single pixel, is that it is frequently located in the most-critical area of the instability and can provide accurate TOF forecasts for the first area to collapse. This is critical in the event the instability does not collapse as a single coherent mass. The benchmark pixel TOF analysis results are then compared with those performed using the 50% deformation increment dataset. This comparison helps validate the TOF results provided by the benchmark pixel while taking into account the time-dependent behaviour of the rock mass over a larger area of the instability.

Figure 4 illustrates the pixels selected for the analysis of the slope failure case study; the outlined area and the pixels in green are those selected for analysis. Note that some "runaway pixels" (erroneous measurements due to sudden large changes in atmospheric conditions) were part of the dataset and were not selected for analysis; these are the blue pixels within the outlined areas in Fig. 4. The benchmark was selected as the first pixel to trigger a slope deformation alarm, which in this case was set by the mine staff as 10 mm of deformation over 4 h. The alarm was triggered approximately 12 h before the slope collapsed. The alarm pixel accrued 69.1 mm of cumulative deformation (since SSR deployment) at the time of the first alarm and this was used for the benchmark deformation. Accordingly, the 50% deformation increment includes all pixels adjacent to the benchmark accruing 34.6 mm (0.5(69.1) mm) or more at the time of the first alarm.

Implementation and removal TARP

The triggering of an alarm will initiate the TARP ("implement TARP" in Fig. 2). During the course of the TOF analysis, an action to "elevate TARP to critical alert level" may be required and emergency response measures invoked if the TOF analysis points to imminent slope collapse. An action to "evaluate removal of TARP" is also included in the procedure (before removing the TARP) to serve as a safeguard to ensure that a thorough assessment of the slope's activity and associated risks have been completed before allowing mine workers and equipment to re-enter the area of the instability. Radar measurements must be combined with conventional monitoring techniques and visual inspection of the unstable area. Relying on radar or any other monitoring dataset alone without a visual inspection is an unsafe practice and could result in a slope hazard being overlooked.

It is important to emphasize that the TOF methodology presented here does not provide TARP recommendations. Each mine should develop and implement their own TARP specific to their operation and pit slope hazard inventory.

Onset-of-acceleration (OOA) determination

After the TARP is initiated, analysis of the radar data is performed. A data filtering method is applied involving averaging the deformation measurements over a moving time period to reduce the noise in the data and provide more accurate and reliable TOF analysis results (see Dick 2013 for details). The OOA is determined next based on four plots

1. *Cumulative deformation versus time* — The cumulative deformation plot represents the amount of slope deformation that has occurred since radar deployment. This can be extracted directly from the ground-based radar measurements without manipulation.
2. *Deformation over a given time period versus time* — The deformation over a moving time period is analogous to how alarms are set with GroundProbe SSR and are calculated using every nth observation

$$d_t = d_i - d_{i-n} \quad (1)$$

where d_t is the deformation over the moving time period, d_i is the most recent deformation, and d_{i-n} is the deformation recorded previously for scan n.
3. *Deformation rate (velocity) versus time* — To reduce the amount of noise in the radar data, deformation rates are to be filtered over a moving time period using every nth observation

$$v_i = \frac{d_i - d_{i-n}}{t_i - t_{i-n}} \quad (2)$$

where v_i is the deformation rate, t_i is the most recent time, d_i is the most recent cumulative deformation, t_{i-n} is the previous time for scan n, and d_{i-n} is the previous cumulative deformation for scan n.
4. *Inverse velocity versus time* — Using the same velocity filters as for the deformation rate versus time, the inverse velocities can be plotted.

It is recommended for plots 2, 3, and 4 that where possible, the data be filtered using both a short time period and a long time period for comparison, for examples of 2 and 12 h, respectively. Filtering over a long time period provides less noisy plots allowing the visualization of long-term data trends and an earlier OOA. Filtering over a short period, although typically noisier, shows short-term trends in the data.

Each of the four plots must be monitored until the end of the acceleration event. An OOA is to be selected for both the

Fig. 3. Theoretical cumulative deformation, deformation rate, and inverse velocity versus time plots illustrating the time of onset-of-acceleration, trend update point, and slope failure.

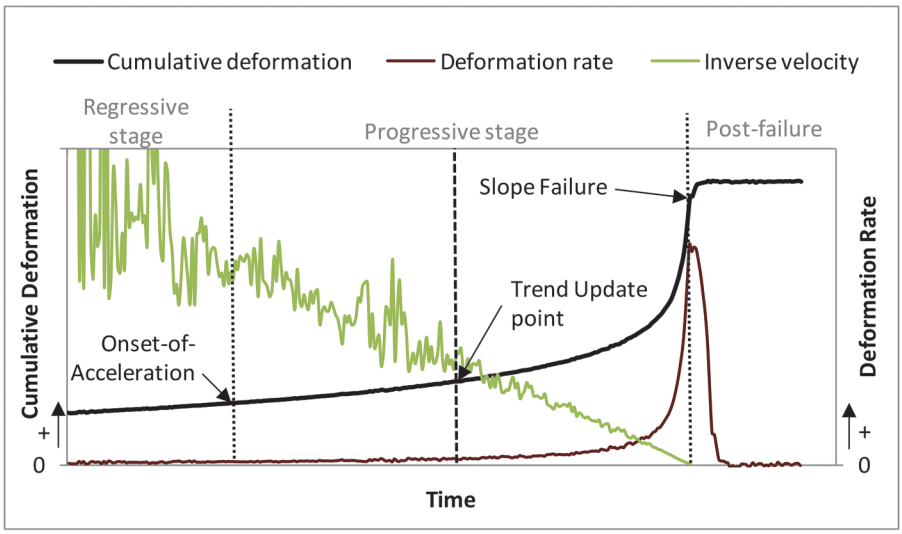

Fig. 4. (*a*) Benchmark pixel and (*b*) 50% deformation increment pixel selections for the copper mine slope failure case study.

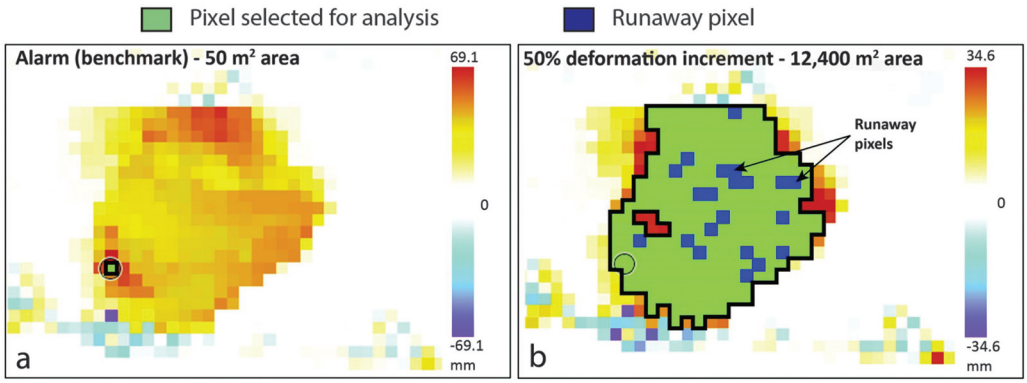

benchmark pixel and the 50% deformation increment datasets. The OOA point for the deformation measurements averaged over multiple pixels provided by the 50% deformation increment dataset may not be the same as the benchmark pixel OOA point due to variations in time-dependent rock mass behaviour throughout the instability. Figure 5 shows an example selection of the OOA where time *t* represents the most recent radar measurement relative to when the radar was deployed.

If an OOA cannot be determined conclusively in the historical data for both the benchmark pixel and the 50% deformation increment datasets, the removal of the mine-specific TARP can be evaluated (see Fig. 2 and discussion in the section titled "Implementation and removal TARP"). If all evidence points to a false alarm, monitoring is to continue as normal.

Time-of-failure (TOF) analysis

The TOF analysis begins if an OOA point can be observed in the historical data. The first step is to apply the inverse-velocity method to the selected OOA points for both the benchmark pixel and 50% deformation increment datasets. The inverse velocities are filtered over both short and long time periods for each data set. The results from these two datasets will be compared alongside each other for the entire procedure. Next, each deformation measurement is cumulatively included up to the current time, plotting each sequential predicted life expectancy on the life-expectancy plot (see Mufundirwa et al. 2010; Dick 2013). Calculating the predicted life expectancy for each sequential deformation measurement provides a record of historical TOF analysis results. With each new deformation measurement provided by the radar, a new predicted life expectancy can be calculated and plotted in real time on the life-expectancy plot, adding to the established historical record. This inverse-velocity analysis from the OOA continues until the end of the acceleration event to monitor the analysis results of the entire dataset relative to the acceleration trend.

If a significant change in the acceleration trend behaviour and (or) a reduction in data noise is observed for either the benchmark pixel or 50% deformation increment datasets, it is advised that additional TOF analyses be undertaken at that point, termed a TU point. This should be conducted in parallel with the inverse-velocity analyses from the original OOA for additional comparison. The rationale behind identifying a TU point is to omit historical data in favour of newer measurements that may give more accurate TOF analysis results, or to identify a temporary or permanent deceleration (stabilization) trend. The TU point is determined through visual inspection in the same way the OOA is selected. The inverse-velocity and SLO TOF analysis methods are to be employed using the data from the benchmark pixel and 50% deformation increment cumulatively including each measurement after the TU point. With each new data point, a new predicted life expectancy can be calculated and plotted on a life-expectancy plot. For clarity, it is advised that the inverse-velocity

Can. Geotech. J. Downloaded from www.nrcresearchpress.com by University of British Columbia on 04/09/15
For personal use only.

Fig. 5. Example of real-time OOA selection using (*a*) time–deformation, (*b*) time–deformation rate, and (*c*) time–inverse-velocity trends.

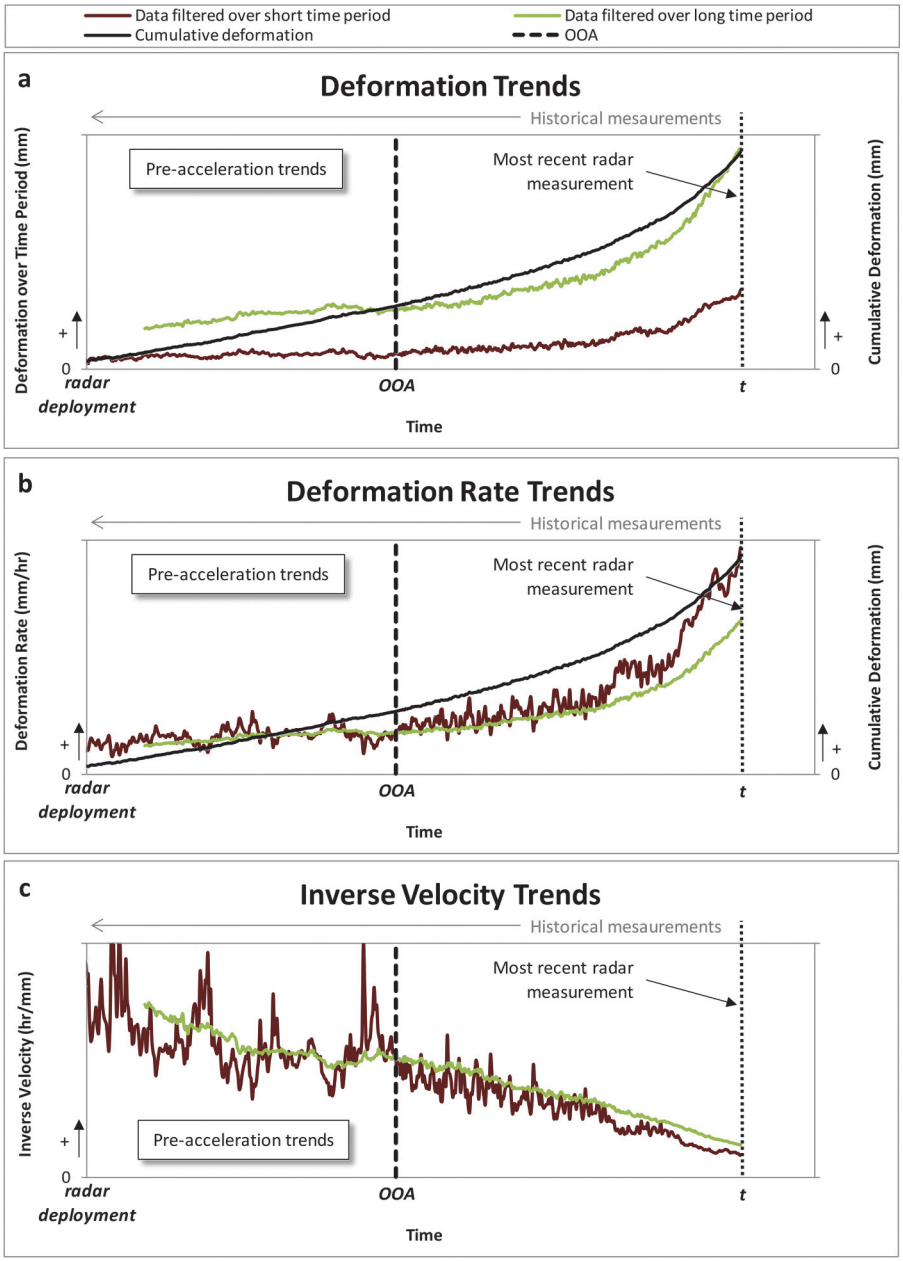

and SLO TOF analysis results be plotted separately for each additional analysis undertaken at a TU point.

Multiple TU points can be selected and additional parallel TOF analyses can be performed at the discretion of the user based on the data specific to each case. This is represented by a loop in the methodology flowchart (Fig. 2). TU points can be selected in the historical data recorded prior to the implementation of the TOF analysis methodology and (or) as new trends develop while executing real-time analyses. If the change in acceleration TU point corresponds to a deceleration in the deformation measurements, this should be apparent in the predicted life expectancy trend and a re-evaluation of the TOF analysis can be conducted; this is discussed in more detail in the section titled "Failure imminence".

Figure 6 shows the deformation, deformation rate, and inverse-velocity trends (filtered over short and long time periods) for the open-pit slope failure case study and illustrates the selected OOA and TU points. For clarification, only one TU point was chosen for each dataset; in this case a decrease in data noise was observed. Note that multiple TU points could have been selected to provide additional result comparisons. As discussed in the section titled "Benchmark pixel and 50% deformation increment selection", the benchmark pixel was established at the time of the first alarm (see "1st alarm" line superimposed on the plot in Fig. 6).

Figure 7 shows the corresponding TOF analysis results for the benchmark pixel and 50% deformation increment data plotted on life-expectancy plots. The inverse-velocity analysis was applied to the data collected from the OOA and TU points onwards, whereas the SLO method was applied to the data from the TU point onwards only. Both the inverse-velocity and SLO results are compared in real time, thus providing multiple predicted life-expectancy results utilizing and omitting different portions of the radar dataset to add confidence in decision-making. Only predicted life expectancies within a converging negative linear trend are considered to be valid and used confidently.

As this was a back-analysis, the actual time of slope collapse was known (approximately 12 h after the triggering of the first alarm).

Can. Geotech. J. Downloaded from www.nrcresearchpress.com by University of British Columbia on 04/09/15
For personal use only.

Fig. 6. (*a*) Cumulative deformation, (*b*) deformation rate, and (*c*) inverse-velocity trends for the copper mine slope failure case study.

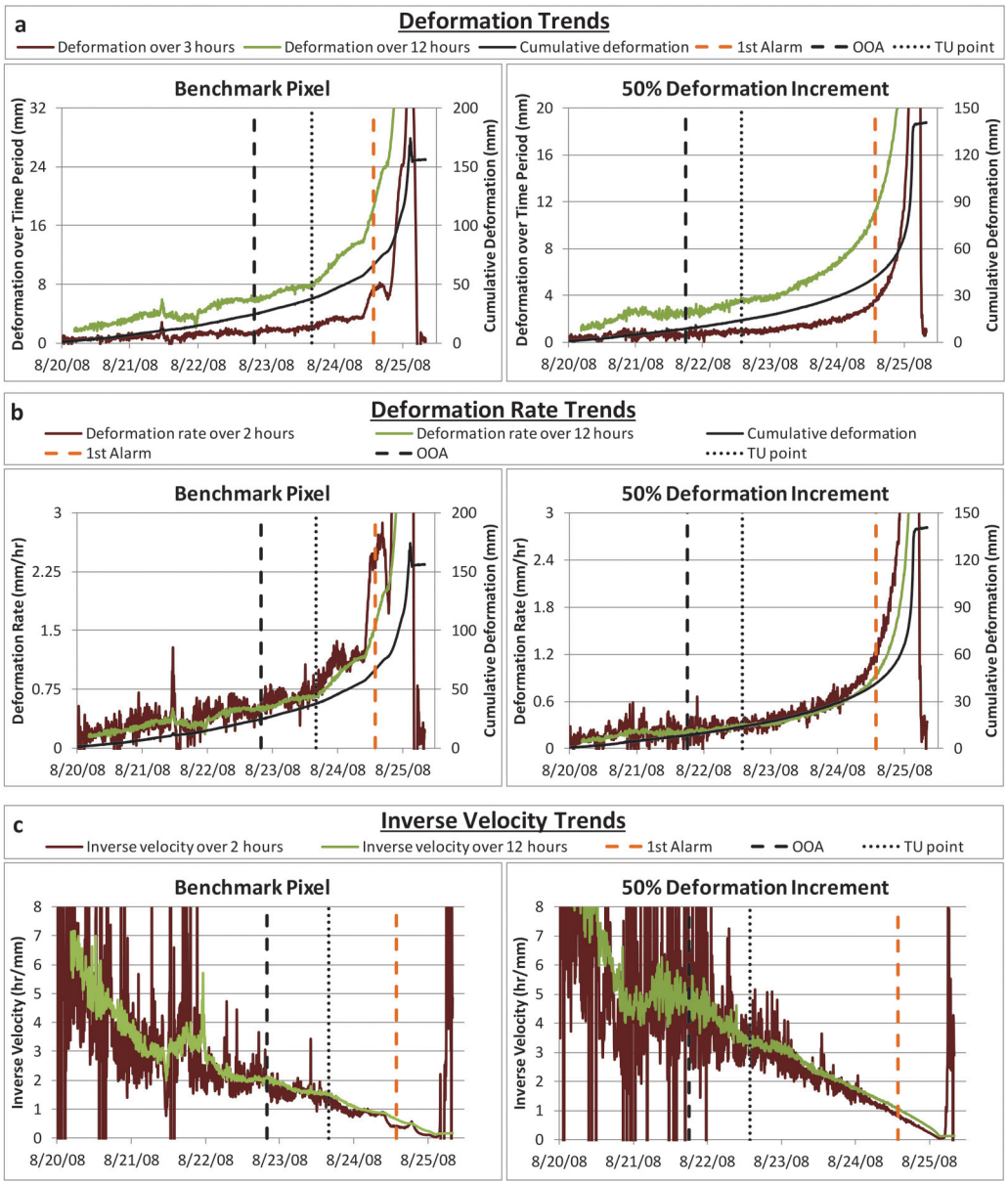

This is represented using an "actual life expectancy" line. The closer the predicted life expectancies are to the actual, the more accurate the TOF analysis results. A predicted life expectancy plotting above the actual represents an overprediction of the TOF at the time the prediction is made. Conversely, a predicted life expectancy plotting below the actual represents an underprediction.

Failure imminence

Once the TOF analysis procedure is in place, the geotechnical engineer must continue to monitor the deformation trends and life expectancy plots as new measurements become available. The predicted life expectancies may begin to show a negative linear trend towards zero, indicating a likelihood of imminent slope failure. However, there are two possible outcomes after the TOF analysis is initiated: (*i*) the instability accelerates and fails (termed a "slope failure event") or (*ii*) the instability decelerates and stabilizes, which is seen as the end of a "temporary acceleration event." The predicted life expectancies for both outcomes may show linear convergence of valid values; however, for a temporary acceleration event this trend will diverge as the instability decelerates. Figure 8 illustrates the typical life expectancy plots for a slope failure event and a temporary acceleration event.

Acceleration event outcomes

During the course of this investigation, which involved the back-analysis of eight slope failures captured by SSR (see Dick 2013), four main acceleration event outcomes were observed. These differ based on the deformation–time trends and collapse characteristics, with each event type representing the outcome of a specific path on the methodology flow chart (Fig. 2). Table 2 lists and defines each acceleration event outcome. These are summarized below. The reader is referred to Dick (2013) for a detailed explanation of each acceleration event outcome and case examples.

If a slope failure occurs, the area of slope collapse is estimated with respect to the area of instability initially identified to determine if the failure was a total collapse event or a partial collapse event. A total collapse is defined as collapse of >90% of the instability area. A partial collapse may or may not be followed by one or

Can. Geotech. J. Downloaded from www.nrcresearchpress.com by University of British Columbia on 04/09/15
For personal use only.

Fig. 7. Copper mine slope failure case study life-expectancy plots for (*a*) inverse-velocity analysis from the OOA, (*b*) inverse-velocity analysis from the TU point, and (*c*) SLO analysis from the TU point.

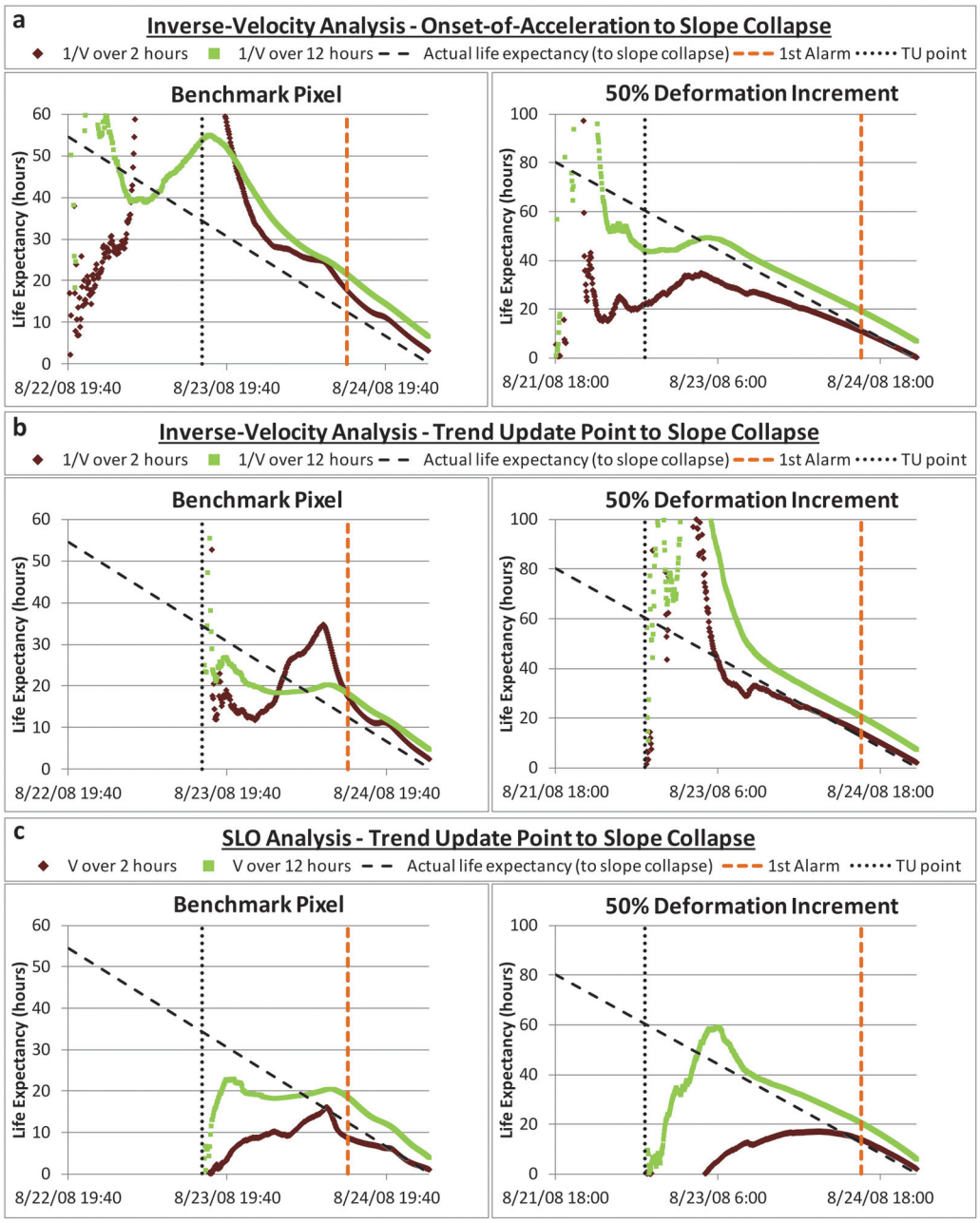

more failure events and is deemed "single" when no further slope collapses occur in the same episode. A staged collapse event involves one or more partial collapses eventually leading to total or near-total collapse of the entire unstable area.

The inverse-velocity and SLO TOF analysis methods can only reliably predict up to the first partial collapse and not the subsequent collapse events. Therefore, once it has been established that a staged collapse event is occurring, continuous monitoring of the deformation, deformation rate, and inverse-velocity trends must be performed to ensure the area is kept clear and no workers re-enter until all subsequent slope collapses occur and the radar measurements show a regressive stage. This is represented by a loop in the methodology flowchart (Fig. 2) following the recognition of a staged collapse event. Once a partial collapse occurs, the observation of new progressive trends in the radar measurements will dictate whether the episode has ended or not. If a new progressive trend is observed, active monitoring of the radar measurements continues until the next collapse event occurs while again ensuring the endangered area is kept clear.

The indicator that the collapse event has ended is the return of post-failure trends to stable pre-failure levels. Averaging the deformation measurements over multiple pixels, such as the 50% deformation increment used in the TOF analysis methodology, must be used to evaluate if a failure event has ended as measurements from single pixels may return to pre-failure trends briefly before "spiking" back to critical levels; in real-time, this may falsely indicate the end of a failure event. In addition to returning to pre-failure levels, post-failure trends will exhibit an increased amount of noise, especially in the inverse-velocity plot.

Post-assessment and evaluation

Reduction of the alarm level or removal of the TARP conditions should only be authorized after a thorough inspection and risk

Can. Geotech. J. Downloaded from www.nrcresearchpress.com by University of British Columbia on 04/09/15
For personal use only.

Can. Geotech. J. Downloaded from www.nrcresearchpress.com by University of British Columbia on 04/09/15
For personal use only.

Fig. 8. Typical life-expectancy plots for a slope failure event and a temporary acceleration event.

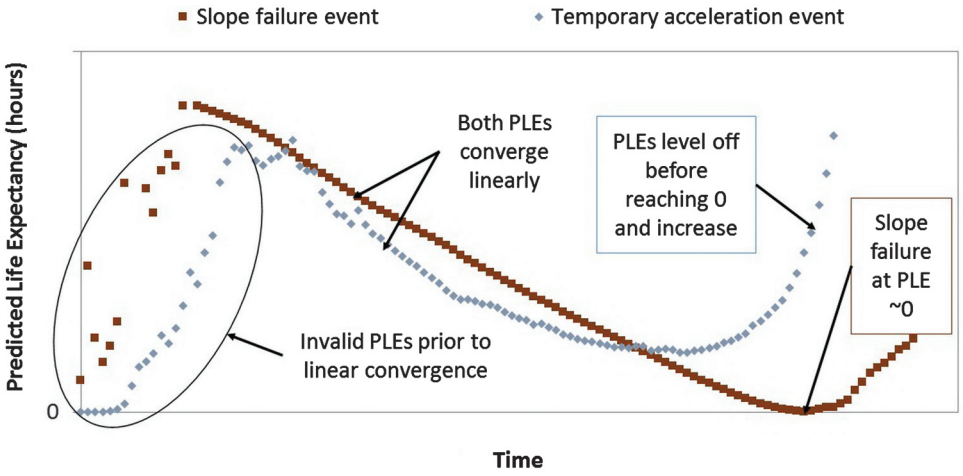

Table 2. Acceleration event outcome definitions.

Event outcome	Definition
Temporary acceleration	The slope demonstrates an accelerating deformation trend but subsequently decelerates and self-stabilizes without collapse.
Total collapse	The slope catastrophically collapses as a single event (>90% of the unstable area) following progressive–accelerating deformation behaviour.
Single partial collapse	Only part of the instability collapses (<90%) as a single event following progressive deformation; no new progressive deformation is observed immediately after the partial collapse.
Staged collapse	Part of the instability collapses (<90%) following progressive deformation, with a new progressive deformation stage being observed immediately after the partial collapse leading to multiple additional slope collapse events.

assessment following the end of the acceleration event. It is also important to assess the performance of the emergency response procedures. Some points to consider when conducting a post-assessment survey following a slope acceleration event are

- Did initiation of a critical alert level allow sufficient time for evacuation of the endangered area?
- Were the trigger thresholds suitable to provide sufficient response time or do they need to be reassessed?
- Did all personnel understand and follow the appropriate TARP or emergency response procedures?
- Did the event expose any flaws in the TARP or emergency response procedures that need to be addressed?
- Were any new indicators of future instabilities recorded during the post-failure visual inspection?

Identifying the successes and areas in need of improvement is essential in the continuous progression and refinement of the TARP and emergency response procedures to ensure worker safety and minimize impact on production schedules.

Discussion

Slope failure case study TOF results

The case study used here to demonstrate the TOF analysis procedure involved a total collapse with failure occurring as a coherent mass in a single event. Figure 9 presents the SSR deformation and coherence image at the time of slope collapse illustrating the estimated area of collapse compared with the estimated area of instability. Low coherence of the pixels within the instability serves as a good indicator of a collapse because the detachment of slope material abruptly increases the range, possibly exposing different rock material with different amplitude characteristics. The deformation, deformation rate, and inverse-velocity trends provided in Fig. 6 also show the signature of a single collapse event, where the progressive trend peaks at the time of slope failure and then returns to a regressive post-failure state.

The primary benefit in this case of averaging the radar measurements over multiple pixels for the 50% deformation increment relative to the single benchmark pixel was the reduction in noise in the dataset. Applying the inverse-velocity and SLO methods to data with less noise increased the reliability and accuracy of the results. When comparing the deformation, deformation rate, and inverse-velocity trends for both pixel selection areas (shown in Fig. 6), the 50% deformation increment dataset provides smoother trends. As a result, the OOA could be identified more than 1 day earlier than for the benchmark pixel data and almost 3 days before the triggering of the first alarm. An earlier OOA selection allowed the application of TOF analyses and as a result the convergence of predicted life expectancies earlier in the dataset. Similarly, a TU point could be chosen earlier in the 50% deformation increment dataset, allowing for additional comparative valid TOF analysis results. Although initiation of the TOF analysis procedure might not occur until the first alarm is triggered, approximately 12 h prior to the actual slope collapse in this case, having a historical record of predicted life expectancies (shown in Fig. 7) indicating a well-established linearly converging trend more than 1 day earlier would allow for more confident judgments regarding the imminence of slope failure.

By filtering the deformation rate measurements over a long time period, in this case 12 h, the OOA could be detected earlier in the data allowing valid predicted life-expectancy trends to be established well before the first alarm trigger (almost 2 days for the 50% deformation increment). However, TOF analysis results using data filtered over a long time period were less accurate and over-predicted the time of slope failure. This was the case for all TOF analysis results for both the benchmark pixel and 50% deformation increment datasets. By including deformation rate measurements filtered over a short period of time, in this case 2 h, the delay in linear convergence of the predicted life-expectancy trends was compensated by more accurate TOF analysis results closer to the actual time of slope failure. Therefore, more reliable TOF analysis results were achieved by combining a long deformation rate

Can. Geotech. J. Downloaded from www.nrcresearchpress.com by University of British Columbia on 04/09/15
For personal use only.

Fig. 9. Cumulative deformation and coherence image of the copper mine slope failure case study as a total collapse event.

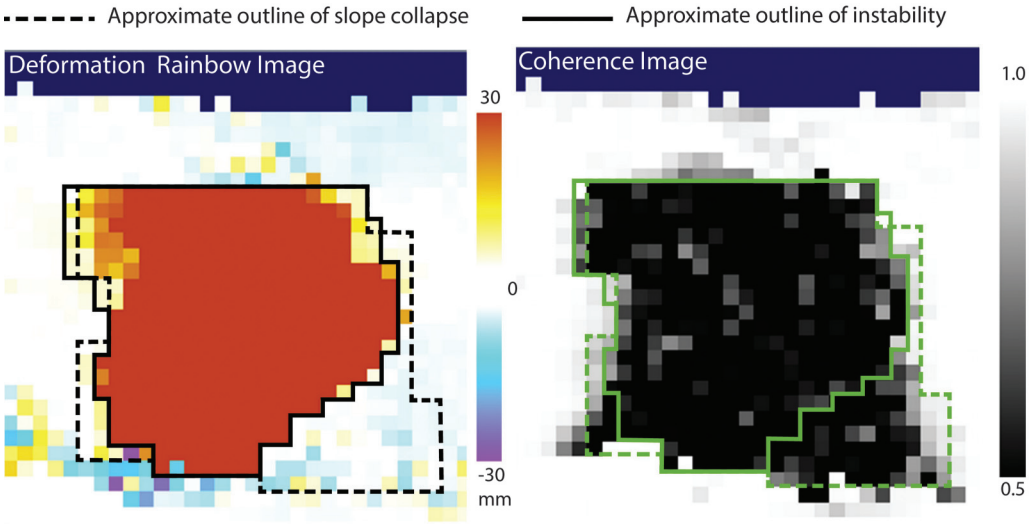

Table 3. Copper mine slope failure case study TOF analysis results.

	Predicted life expectancy (h)							
	Benchmark pixel				50% deformation increment			
Actual life expectancy (h)	Max	Min	Median	Average	Max	Min	Median	Average
48	N/P	N/P	N/P	N/P	53	35	49	45
36	N/P	N/P	N/P	N/P	46	27	39	37
24	35	19	28	29	32	17	27	25
12 (alarm)	21	8	17	17	20	11	16	16
6	14	6	11	11	14	6	11	10

time period filter to establish earlier valid predicted life-expectancy trends and a short deformation rate time period filter providing more accurate results closer to slope failure.

Both the inverse-velocity and SLO methods were used for TOF analysis beginning from the TU point. Based on the linear convergence time of the predicted life expectancies and the accuracy of the prediction compared with the actual time of slope collapse, the inverse-velocity method gave better results than the SLO method for the 50% deformation increment dataset while the SLO method gave better results for the single benchmark pixel dataset. As a result, more dependable results were achieved by using and comparing both TOF analysis methods.

Table 3 summarizes the accuracy of the predicted life-expectancy results for the benchmark pixel and 50% deformation increment datasets compared with the time of actual slope collapse (actual life expectancy); N/P indicates a valid predicted life expectancy result was not yet resolved. The benchmark pixel and 50% deformation increment TOF results began giving valid results 35 and 50 h prior to actual slope collapse, respectively. Table 3 includes the results for all valid predicted life expectancies from the TOF analyses beginning from the OOA and subsequent TU points over both short and long filtration time periods. This produced six predicted life-expectancy trends for each dataset (12 in total). The median is the calculated valid predicted life expectancy separating the higher half from the lower half at the specified actual life expectancy. The average is the arithmetic mean between all calculated valid predicted life expectancies at the specified actual life expectancy (not between the maximum and minimum value).

Overall, the TOF analyses slightly overpredicted the actual time of slope collapse, as illustrated in Fig. 7 where the majority of the predicted life expectancies are above the actual life-expectancy line. This overprediction is also shown by the results in Table 3 where most median and average values are above the actual life expectancy. However, in all cases the minimum value was equal to or below the actual life expectancy. Therefore, even though the majority of the TOF analysis results were overpredictions, each case still provided a safe lower bound measurement.

Reliability and performance of the real-time TOF analysis methodology

A limitation of the proposed TOF analysis methodology is the requirement of the user to visually select the OOA to begin the TOF analyses. This introduces subjectivity as different geotechnical engineers may choose different OOA points depending on their individual experience and judgement. A sensitivity analysis regarding this issue was performed by Dick (2013), and showed that the variation in TOF results for the deformation rates filtered over a shorter time period (e.g., 2 h) produced larger variations in predicted life expectancies compared to filters involving longer time periods (e.g., 12 h). Figure 10 summarizes the results of the sensitivity analysis. These results also show that earlier OOAs provided no valid or accurate predicted life expectancies; later OOAs provided valid and reasonably accurate predicted life expectancies early in the data, but slightly overpredicted the actual time of collapse. This suggests that the more conservative approach is to select the OOA later rather than earlier when the actual OOA might not be well-defined in the radar measurements.

In terms of reliability, utilizing both the benchmark pixel and 50% deformation increment datasets was seen to provide more reliable and accurate TOF analysis results. By comparison, selecting random pixels for the different case studies returned significantly poorer results in terms of predicted life expectancies and

Fig. 10. Results from OOA sensitivity analysis for open-pit mine slope failure case history, comparing different time windows for data filtering applied to the 50% deformation increment dataset using the inverse-velocity method: (*a*) inverse-velocity trends showing OOA selections; (*b*) life-expectancy plots for TOF analyses undertaken at each OOA.

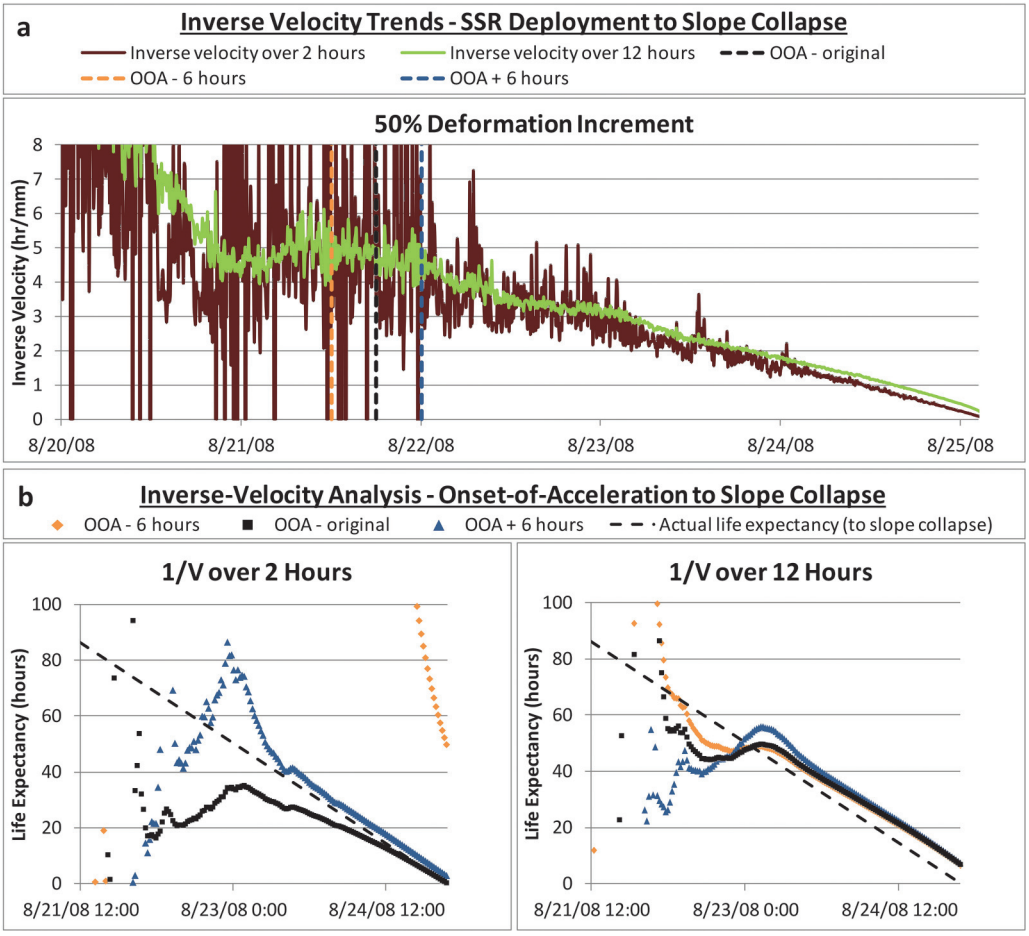

Fig. 11. SSR deformation image at the time of the first alarm for a single partial instability collapse, showing the location of the different single pixels tested in Fig. 12 against the 50% deformation increment: (*a*) single pixel selections; (*b*) pixels included in the 50% deformation increment.

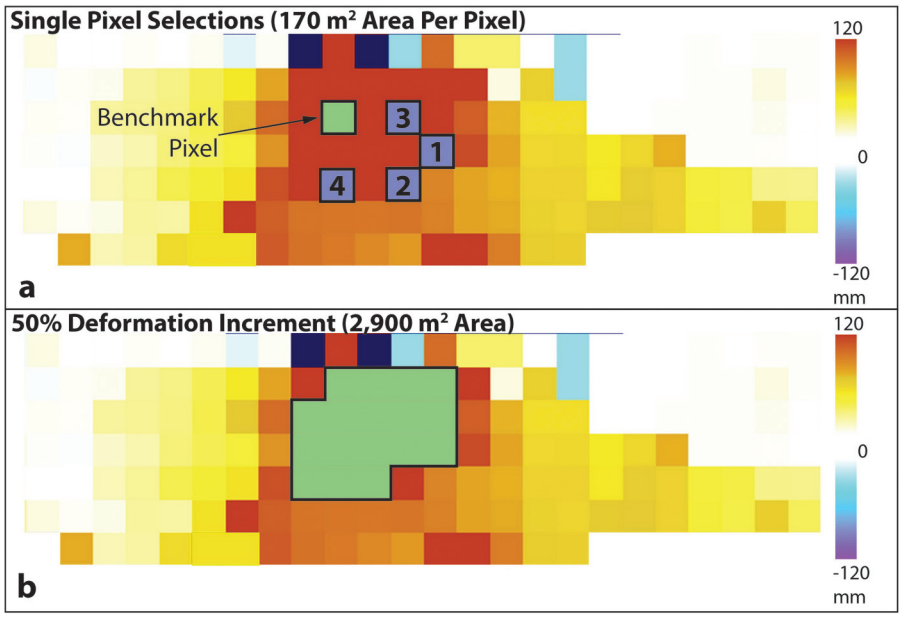

Can. Geotech. J. Downloaded from www.nrcresearchpress.com by University of British Columbia on 04/09/15
For personal use only.

Fig. 12. Inverse-velocity trends for a single partial instability collapse, comparing the predictions for a single versus multiple pixel TOF analysis. See Fig. 11 for the location of the pixels relative to outline of instability.

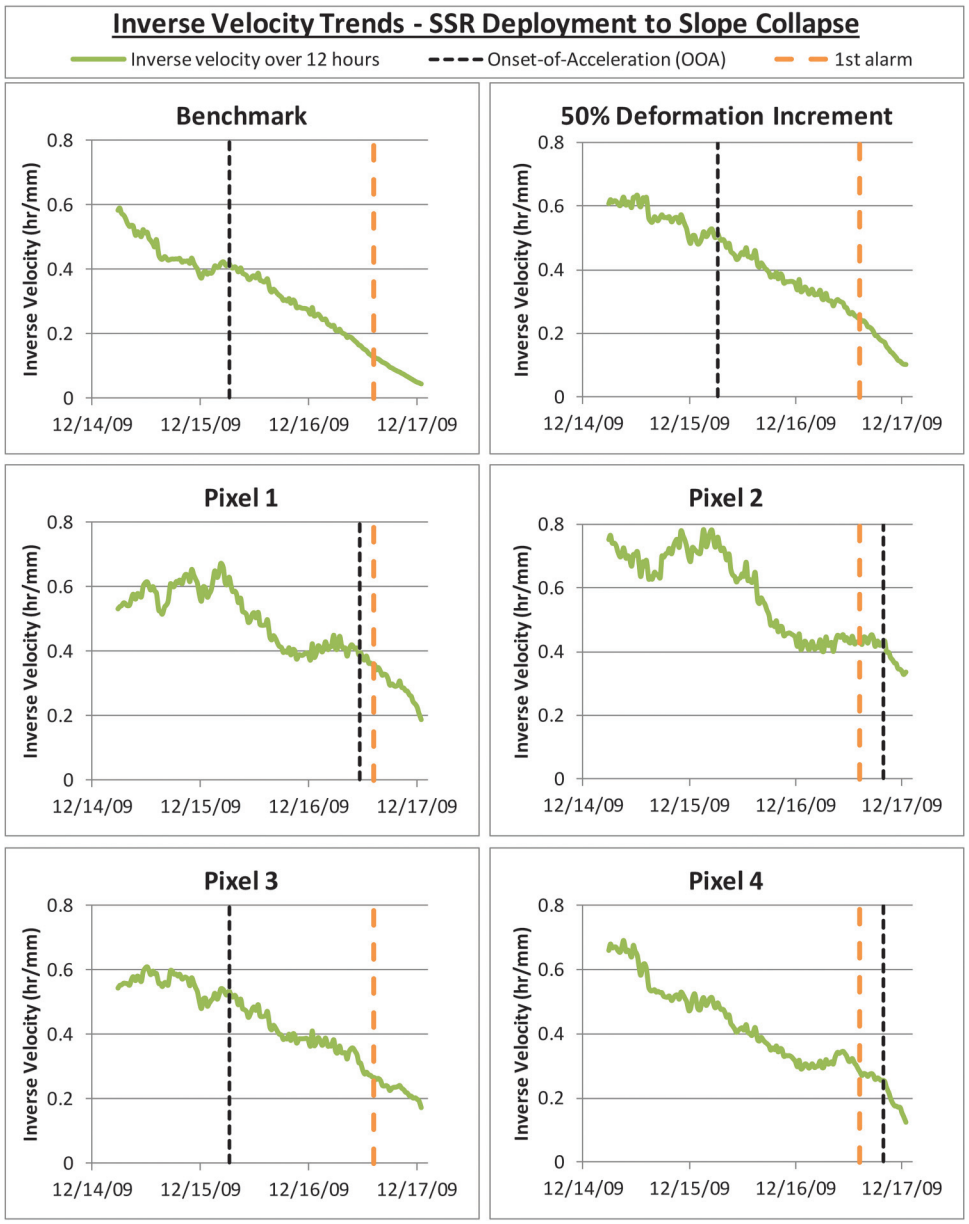

TOF for the back-analyzed slope collapses (see Dick 2013). Overall, TOF analyses using a 50% deformation increment versus randomly selected single pixels provided an earlier predicted life-expectancy trend indicating imminent slope failure.

Averaging the deformation trends over a larger area within the bounds of the instability versus relying on single pixels was also seen to be especially important when the TOF analyses involve a partial or staged collapse event. Figure 11 shows the location of several randomly selected individual pixels compared with the benchmark pixel and 50% deformation increment pixels for one of the case studies analyzed (see Dick 2013 for details). Figure 12 shows the corresponding inverse-velocity trends. The variation in data trends is considerable, despite the single pixels being selected in close proximity to each other within the region showing the highest cumulative deformation. It was found in the case of partial instability collapses (resulting in either a single or staged partial collapse event) that the benchmark pixel will provide more accurate TOF analysis results, compared to other single pixels, because it is commonly located in the area of the instability with the greatest likelihood of collapsing first.

Concluding remarks

Slope failures captured by GroundProbe SSR at eight major open-pit mining operations were examined in detail, leading to the development of a new methodology for real-time TOF analysis for open-pit mine slopes being monitored using ground-based radars. Two TOF analysis methods developed for conventional geodetic monitoring are employed in the proposed methodology: the inverse-velocity method (Fukuzono 1985) and the SLO method (Mufundirwa et al. 2010). The proposed methodology is intended to be incorporated into a mine's existing TARP and initiated when a slope deformation alarm is triggered and (or) an accelerating deformation trend is observed. Four acceleration event outcomes were defined based on the back-analyzed slope failure cases investigated in this study: (*i*) temporary acceleration, (*ii*) total collapse, (*iii*) single partial collapse, and (*iv*) staged collapse.

Can. Geotech. J. Downloaded from www.nrcresearchpress.com by University of British Columbia on 04/09/15
For personal use only.

Can. Geotech. J. Downloaded from www.nrcresearchpress.com by University of British Columbia on 04/09/15
For personal use only.

Incorporated into the proposed methodology is a new systematic multi-pixel selection technique termed the "percent deformation method." The basis of the percent deformation method is the use of a benchmark pixel to select multiple surrounding pixels based on a percentage of its deformation. The benchmark pixel can be selected as the pixel that triggered the slope deformation alarm or as the pixel that has accumulated the highest cumulative deformation during an acceleration event. The latter allows for the analysis to be initiated without the triggering of a slope deformation alarm (i.e., it is independent of the early-warning alarm threshold set by a particular operation). When multiple pixels are selected, the deformation trends are averaged over all of the pixels chosen.

The proposed methodology involves a simultaneous, real-time comparison of the TOF analysis results for the benchmark pixel and 50% deformation increment datasets. This is shown to provide a more robust, reliable, and accurate set of results in the following ways:

- Averaging the deformation measurements over multiple pixels can provide smoother, less noisy trends resulting in improved TOF analysis results.
- Benchmark pixel data can perform well for partial collapse events as they typically coincide with the most critical area of the instability.
- Analyzing deformation measurements averaged over a large area of the instability is essential in understanding the overall time-dependent behaviour of the rock mass, especially for a staged collapse event.
- Actively comparing the benchmark and 50% deformation increment datasets provides more TOF analysis results to help improve decision confidence.

The following general guidelines are suggested when applying the proposed real-time TOF analysis methodology:

- Radar data should be filtered over a long time period (e.g., 12 h) to establish an early OOA point and a short time period (e.g., 2 h) to provide more accurate TOF analysis results closer to failure. The time period length is dependent on the amount of measurement data available prior to initiating the TOF analyses.
- If the OOA point is not clearly identifiable, it is more conservative to select a later rather than earlier time point in the dataset.
- The inverse-velocity and SLO TOF analysis methods are recommended because they utilize linear regression that is easily applied to time-deformation measurements.
- Using life-expectancy plots as a tool when conducting TOF analyses is recommended as they provide a historical record of previous TOF analysis results, are easily updated in real-time when new results are calculated, and provide a visual aid when determining if slope failure is imminent.
- Conducting parallel TOF analyses at TU points in addition to those referenced at the OOA provides additional comparative TOF analysis results to help improve decision confidence.
- Continuous monitoring should be carried out for all deformation, deformation rate, and inverse-velocity trends in conjunction with life-expectancy plots.

In summary, utilizing deformation measurements from a systematically chosen single pixel in addition to deformation measurements averaged over multiple pixels over the instability can provide accurate and reliable TOF analysis results. It is hoped that future implementation of the proposed real-time TOF analysis methodology will reduce uncertainty and aid geotechnical engineers responsible for maintaining safe mine operations in relation to pit slope stability. The application of the developed methodology is not restricted to open-pit mines and can be utilized for other rock slope hazards where radar monitoring is employed, such as those threatening transportation corridors and landslides above dams. Implementation of this methodology will further position ground-based radar slope monitoring technology as a vital tool in critical rock slope stability monitoring for ensuring workplace safety and minimizing impact on mine production schedules.

Acknowledgements

The authors would like to thank David Noon and GroundProbe for their time and effort in providing SSR datasets for this research. Our gratitude is also extended to the mining companies who agreed to allow us to use their data. Funding for this research was provided in part through a British Columbia Innovation Council Natural Resources and Applied Sciences (NRAS) Endowment grant.

References

Armstrong, J., and Rose, N.D. 2009. Mine operation and management of progressive slope deformation on the south wall of the Barrick Goldstrike Betze-Post Open Pit. *In* Slope Stability 2009: Proceedings of the International Symposium on Rock Slope Stability in Open Pit Mining and Civil Engineering, Santiago.

Cahill, J., and Lee, M. 2006. Ground control at Leinster Nickel operations. *In* Proceedings of the International Symposium of Rock Slopes in Open Pit Mining and Civil Engineering, Cape Town, South Africa. The South African Institute of Mining and Metallurgy. pp. 321–334.

Crosta, G.B., and Agliardi, F. 2003. Failure forecast for large rock slides by surface displacement measurements. Canadian Geotechnical Journal, **40**(1): 176–191. doi:10.1139/t02-085.

Day, A.P., and Seery, J.M. 2007. Monitoring of a large wall failure at Tom Price iron ore mine. *In* Proceedings of the International Symposium on Rock Slope Stability in Open Pit Mining and Civil Engineering, Perth, Australia. Australian Centre for Geomechanics. pp. 333–340.

Dick, G.J. 2013. Development of an early warning time-of-failure analysis methodology for open pit mine slopes utilizing the spatial distribution of ground-based radar monitoring data. M.A.Sc. thesis, The University of British Columbia, Vancouver, BC.

Dick, G.J., Eberhardt, E., Stead, D., and Rose, N.D. 2013. Early detection of impending slope failure in open pit mines using spatial and temporal analysis of real aperture radar measurements. *In* Proceedings of Slope stability 2013. Australian Centre for Geomechanics, Brisbane, Australia. pp. 949–962.

Doyle, J.B., and Reese, J.D. 2011. Slope monitoring and back analysis of east fault failure, Bingham Canyon Mine, Utah. *In* Proceedings of Slope Stability 2011: International Symposium on Rock Slope Stability in Open Pit Mining and Civil Engineering. Canadian Rock Mechanics Association, Vancouver, B.C.

Fukui, K., and Okubo, S. 1997. Life expectancy and tertiary creep for rock. *In* Proceedings of the Fall Meeting Mining and Minerals Processing Institute of Japan. pp. 91–94.

Fukuzono, T. 1985. A new method for predicting the failure time of a slope. *In* Proceedings of the Fourth International Conference and Field Workshop on Landslides, Tokyo, Japan. Japan Landslide Society. pp. 145–150.

Ginting, A., Stawski, M., and Widiadi, R. 2011. Geotechnical risk management and mitigation at Grasberg Open Pit, PT Freeport Indonesia. *In* Proceedings of Slope Stability 2011: International Symposium on Rock Slope Stability in Open Pit Mining and Civil Engineering. Vancouver, BC. Canadian Rock Mechanics Association.

GroundProbe Pty Ltd. 2012. SSRViewer 5.4 user manual. Brisbane, Australia.

Harries, N.J., and Cabrejo, A.G.L. 2010. Deformation response of coal mine slopes - implications for slope hazard management using evacuation based on slope monitoring. *In* Proceedings of the 44th US Rock Mechanics Symposium and 5th U.S.–Canada Rock Mechanics Symposium. American Rock Mechanics Association, Salt Lake City, Utah.

Harries, N.J., and Roberts, H. 2007. The use of Slope Stability Radar (SSR) in managing slope instability hazards. *In* Rock Mechanics: Meeting Society's Challenges and Demands, Proceedings of the 1st Canada–US Rock Mechanics Symposium, Vancouver. Taylor & Francis, London. pp. 53–60. doi:10.1201/NOE0415444019-c7.

Harries, N., Noon, D., and Rowley, K. 2006. Case studies of slope stability radar used in open cut mines. *In* Proceedings of Stability of Rock Slopes in Open Pit Mining and Civil Engineering Situations, Johannesburg, South Africa. SAIMM. pp. 335–342.

Jones, E., Andrews, P., and Holley, S. 2011. The Wallaby Mine: Maintaining pit wall stability for continued underground mining. *In* Proceedings of Slope Stability 2011: International Symposium on Rock Slope Stability in Open Pit Mining and Civil Engineering. Canadian Rock Mechanics Association, Vancouver, BC.

Little, M.J. 2006. Slope monitoring at PPRust open pit operation. *In* Proceedings of the International Symposium on Stability of Rock Slopes in Open Pit Mining and Civil Engineering, Johannesburg, South Africa. Symposium Series S44 and Metallurgy. The South African Institute of Mining. pp. 211–230.

Macqueen, G.K., Salas, E.I., and Hutchison, B.J. 2013. Application of radar monitoring at Savage River Mine, Tasmania. *In* Proceedings of Slope stability 2013. Australian Centre for Geomechanics, Brisbane, Australia. pp. 1011–1020.

Mercer, K.G. 2006. Investigation into the time dependent deformation behaviour and failure mechanisms of unsupported rock slopes based on the interpretation of observed deformation behaviour. Ph.D. thesis, University of Witwatersrand, Johannesburg, South Africa.

Mufundirwa, A., Fujii, Y., and Kodama, J. 2010. A new practical method for prediction of geomechanical failure-time. International Journal of Rock Mechanics and Mining Science, **47**: 1079–1090. doi:10.1016/j.ijrmms.2010.07.001.

Read, J., and Stacey, P. 2009. Guidelines for open pit slope design.CSIRO Publishing, Collingwood, VIC, Australia.

Reeves, B., Noon, D., Stickley, G., and Longstaff, D. 2001. Slope stability radar for monitoring mine walls. *In* Proceedings of SPIE. pp. 57–67. doi:10.1117/12.450188.

Rose, N.D., and Hungr, O. 2007. Forecasting potential rock slope failure in open pit mines using the inverse-velocity method. International Journal of Rock Mechanics & Mining Science, **44**: 308–320. doi:10.1016/j.ijrmms.2006.07.014.

Venter, J., Kuzmanovic, A., and Wessels, S.D.N. 2013. An evaluation of the CUSUM and inverse velocity methods of failure prediction based on two open pit instabilities in the Pilbara. *In* Slope stability 2013. Australian Centre for Geomechanics, Brisbane, Australia. pp. 1061–1076.

Yang, D.Y., Mercer, R.A., Brouwer, K.J., and Tomlinson, C. 2011. Managing pit slope stability at the Kemess South Mine - changes over time. *In* Proceedings of Slope Stability 2011: International Symposium on Rock Slope Stability in Open Pit Mining and Civil Engineering. Canadian Rock Mechanics Association, Vancouver, BC.

Zavodni, Z.M., and Broadbent, C.D. 1980. Slope failure kinematics. Bulletin, Canadian Institute of Mining. pp. 69–74.

Can. Geotech. J. Downloaded from www.nrcresearchpress.com by University of British Columbia on 04/09/15
For personal use only.